

Thermal conductivity and thermoelectric power of titanium carbide single crystals

Donald T. Morelli

Physics Department, General Motors Research Laboratories, Warren, Michigan 48090-9055

(Received 29 March 1991)

We have studied the thermal conductivity and thermoelectric power of single crystals of titanium carbide (TiC_x). This material crystallizes in the sodium chloride structure for a range of stoichiometries. We have investigated samples with $x=0.88, 0.93,$ and 0.95 . The thermal conductivity contains both a lattice (phonon) and an electronic component. Near room temperature the electronic component, as estimated from the Wiedemann-Franz law, comprises up to 25% of the total heat conduction in this system, but this value decreases as the temperature is lowered, and below 100 K nearly all of the heat is carried by lattice vibrations. Though not playing a direct role in the heat conduction at low temperatures, the carriers are nevertheless effective scatterers of lattice vibrations in this regime and are primarily responsible for limiting the phonon thermal conductivity below 100 K. At higher temperatures, the lattice conductivity is limited mainly by carbon-vacancy scattering and phonon-phonon umklapp processes. The thermopower of these crystals deviates significantly from that expected for a simple electron-diffusion process. This behavior is shown to be quantitatively consistent with scattering of the s -band transport electrons into d states as described by Mott's model of transport in transition metals.

INTRODUCTION

Transition-metal carbides and nitrides are very interesting materials from both technological and fundamental viewpoints. On the one hand, they are all high-melting-point, ultrahard materials with good thermal and electrical properties. On the other hand, many members of this family are superconductors with transition temperatures as high as 18 K.

Though not a superconductor, titanium carbide (TiC_x) is a rather well studied member of this class. Single crystals of this material form in the rocksalt structure over a fairly wide range of stoichiometry.¹ Earlier workers^{2,3} observed that the electrical resistivity falls from a maximum value of approximately $200 \mu\Omega \text{ cm}$ near $x=0.7$ to $100 \mu\Omega \text{ cm}$ near $x=0.95$ and showed that the electron mobility is inversely proportional to vacancy concentration. Radosevich and Williams^{4,5} measured the thermal conductivity of single crystals spinning a range of compositions below 80 K and observed that the thermal conductivity *decreased* with increasing x . The only other data on a thermal conductivity are those of Taylor⁶ on polycrystalline samples above room temperature. Lye⁷ measured the thermoelectric power on single crystals spanning the range $x=0.79-0.95$, but his study was confined to the temperature range above 100 K. Thus there are significantly large temperature ranges in which many of the thermal transport properties of this material have not been studied.

In this report we present results on the thermal conductivity and thermoelectric power of TiC_x single crystals from 15 K to 300 K. Our thermal conductivity data are the first to cover the range between 80 K and 300 K, and our thermopower data are the first to extend to below 100 K. We find that these results shed important light on the electron-phonon, electron-vacancy, and phonon-vacancy interactions in this system.

EXPERIMENTAL TECHNIQUE

We obtained TiC_x single crystals from Hughes Research Laboratories. An x-ray diffractogram of one of our samples is shown in Fig. 1. A single peak is observed at $2\theta=41.7^\circ$, which indexes to the [200] peak in TiC.

For transport measurements samples were cut in the form of parallelepipeds (with dimensions given in Table I) using a high-speed diamond saw. Electrical resistivity was measured using the four-probe dc technique by epoxying silver wires onto the samples using conductive silver epoxy.⁸ Excitation currents were in the range 1–100 mA, and voltages were measured using a Keithley model 181 nanovoltmeter. We estimate that the absolute uncertainty in our measurement of the electrical resistivity is about 5%, owing largely to the inaccuracy in determining the distance between voltage probes.

In order to measure thermal conductivity and thermoelectric power, a small metal film heater was glued to one end of the sample using thermally conductive epoxy,⁹ with the other end of the sample glued to a temperature-controlled copper block. A temperature difference be-

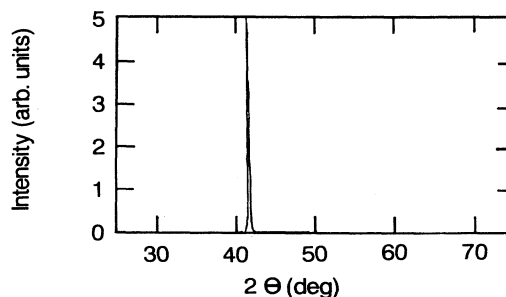


FIG. 1. X-ray diffractogram of a titanium carbide single crystal along a [100] face.

tween two points along the sample length is sensed using a chromel-constantan thermocouple that is epoxied to, but electrically insulated from, the sample at the two points. A second thermocouple is glued at the midpoint of the sample to determine its average temperature with respect to the copper block. Thermal voltages are sensed with a Keithley model 181 nanovoltmeter. A measurement of the thermopower with this method naturally includes a contribution from the leads that must be subtracted from the measured value. We use very thin (0.2 mm) high-purity Pb leads, the absolute thermopower of which has been measured and tabulated by Roberts.¹⁰ We estimate that the absolute errors in the thermal conductivity and thermopower are not more than 5%

RESULTS

Electrical resistivity

Table I contains our results on the room-temperature electrical resistivity and the residual resistivity ratio (RRR) (defined as the ratio of the room-temperature resistivity to that at 10 K) for our three TiC_x samples. Despite the fact that these samples are single crystals, we note the relatively large value of resistivity and its relatively weak temperature dependence. These observations are consistent with previous results,^{2,3} which show that scattering by vacancies (which is an energy-conserving and temperature-independent scattering process) predominantly limits the electrical conduction in these materials. A relationship between resistivity and carbon content in these materials is well established.^{2,3} By comparing our results with those of earlier workers, we can establish the nominal carbon content of our samples; the result is given in Table I. Scattering of electrons by phonons produces an electrical resistivity that increases with increasing temperature, according to the Bloch-Grüneisen law, and this increase is largely masked by the large background resistivity due to vacancy scattering. We shall see below that the predominance of vacancy scattering over phonon scattering has profound consequences for the thermopower of these materials.

Thermal conductivity

In Fig. 2 we display our results for the thermal conductivity as well as those of Radosevich and Williams⁴ below 80 K. It can be seen that our results agree favorably with those of Ref. 4 in the overlap regime, and confirm the interesting trend that at low temperatures the thermal conductivity increases with decreasing x . We observe a peak in the thermal conductivity near 100 K, and a weak fall-

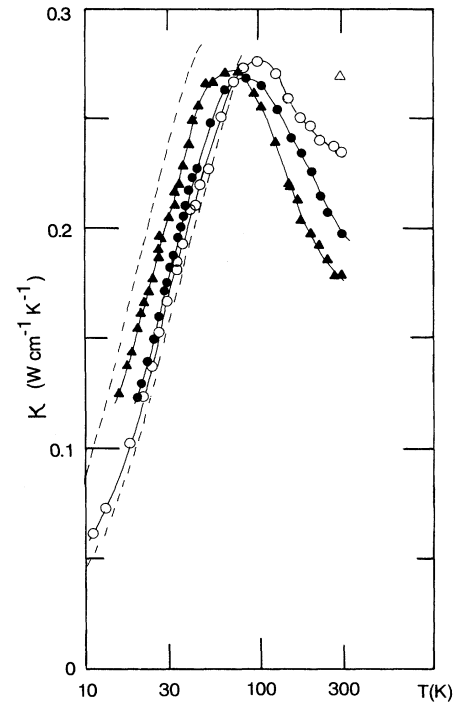


FIG. 2. Thermal conductivity of TiC_x single crystals. Dashed lines represent the result of Ref. 4: the lower line is $x=0.96$ and the upper line in $x=0.86$. Sample designation: \blacktriangle , $x=0.88$; \bullet , $x=0.93$; \circ , $x=0.95$; \triangle , Taylor's polycrystal.

off at higher temperatures. We note that this decline is stronger in the less stoichiometric samples, and that for the sample with $x=0.95$ the thermal conductivity flattens noticeably. At room temperature the thermal conductivity of our single crystals is 15–30% smaller than that of Taylor's polycrystalline sample.⁶

Thermopower

Figure 3 displays the thermoelectric power of our samples. Several striking features are evident. First, we note the slight dependence of the thermopower on stoichiometry, unlike the behavior of the electrical and thermal conductivities. The room-temperature values of $6.0\text{--}6.4 \mu\text{V K}^{-1}$ are essentially independent of carbon content in this stoichiometry range, to within the absolute accuracy of our measurement. Perhaps the most notable feature of the thermopower, however, is its strong nonlinearity with temperature. It is well known

TABLE I. Parameters of TiC_x single crystals; ρ and κ_e are the room-temperature electrical resistivity and electronic thermal conductivity, respectively, and RRR is the residual resistivity ratio.

Sample No.	x	Dimensions (mm ³)	$\rho(300 \text{ K})$ ($\mu\Omega \text{ cm}$)	RRR	$\kappa_e(300 \text{ K})$ ($\text{W cm}^{-1} \text{ K}^{-1}$)
1	0.88	$11.2 \times 4.5 \times 0.8$	204	1.05	0.036
2	0.93	$7.2 \times 2.5 \times 1.4$	133	1.11	0.055
3	0.95	$9.5 \times 2.8 \times 1.6$	126	1.35	0.058

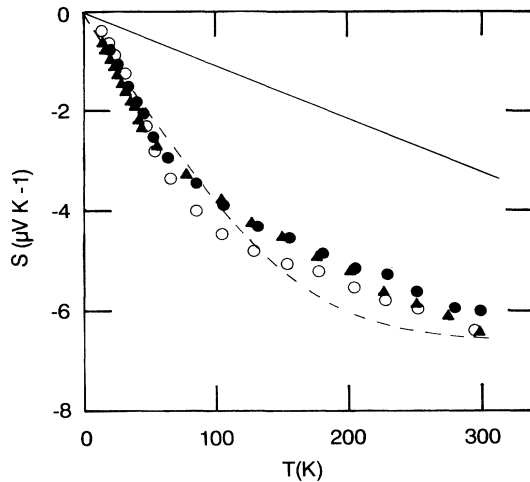


FIG. 3. Thermoelectric power of three TiC_x single crystals. Sample designation is given in Fig. 2. The dashed line is a fit to the data using electron-phonon renormalization; the solid line represents the bare thermopower $X_B T$.

that phonon-drag effects in crystalline materials can produce large anomalies in the thermopower. We reject this as the cause of our hump-shaped curves for several reasons. First, phonon drag is very sensitive to sample quality; it is highly unlikely that samples with even slightly different compositions would exhibit nearly exactly the same phonon-drag thermopower. Furthermore, the high electrical resistivity of our samples indicates that the electrons are much more strongly scattered by vacancies than by phonons; on the other hand, as is argued below, the thermal conductivity data suggest that for $T > 100$ K the phonon mean free path is limited mainly by U processes and defect scattering, which would tend to suppress strongly any phonon-drag effects at higher temperature. Based on these arguments we conclude that the thermopower is completely in the diffusion regime, with phonon-drag effects playing little, if any, role. We must therefore call on another mechanism to explain the interesting thermopower we observe.

DISCUSSION

It is evident from both the electrical resistivity and thermal conductivity that electron-vacancy, phonon-vacancy, and phonon-electron interactions all play significant roles in determining the properties of titanium carbide crystals. This interplay is nicely displayed in the thermal conductivity where at high temperatures κ increases with increasing x while at low temperatures it decreases with increasing x . Radosevich and Williams pointed out⁴ that this latter behavior arises due to an increase in carrier density with decreasing x . They conjecture that these electrons contribute little to the electrical conductivity because they go into the p or d states, but are nonetheless capable of scattering phonons and give rise to the inverse dependence of κ on x at low temperature.

While both phonons and electrons can carry heat, experiment measures the total thermal conductivity

$$\kappa = \kappa_e + \kappa_p, \quad (1)$$

where κ_e represents the electronic thermal conductivity and κ_p represents the phonon, or lattice, thermal conductivity. Because electrons are scattered predominantly by vacancies, a process that is energy conserving from the electrons' point of view, we can use the Wiedemann-Franz law with the free-electron value of the Lorenz ratio to estimate κ_e . The result at room temperature is given in Table I. In the sample with $x=0.95$, electrons carry nearly one-quarter of the heat at room temperature. This fraction falls off with decreasing temperature such that below 100 K the electronic contribution is less than 5%. By subtracting the estimated electronic component we can determine the lattice thermal conductivity; the result is shown in Fig. 4. We see that above 100 K the curves are bunched much more closely together and exhibit nearly the same temperature dependence; however, the absolute magnitude of κ_p still scales with x . The spreading out of the total thermal conductivity curves near room temperature (Fig. 2) is thus due to differing amounts of electronic thermal conductivities. In fact, Taylor's result⁶ of $\kappa=0.27 \text{ W cm}^{-1} \text{ K}^{-1}$ at 300 K may be due to a larger contribution of κ_e in his sample, which

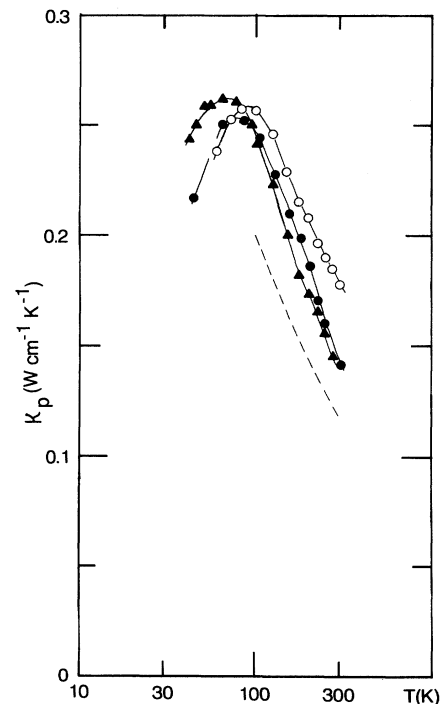


FIG. 4. Lattice thermal conductivity of TiC_x single crystals determined by subtracting the electronic component calculated from the Wiedemann-Franz law from the total thermal conductivity. Solid lines are guides to the eye; the dashed line is the theoretical prediction of the temperature dependence of lattice thermal conductivity in the presence of strong point-defect scattering. For sample designation, see Fig. 2.

was polycrystalline with $x=0.95$. While it may seem counterintuitive that a polycrystalline sample would have a larger electronic thermal conductivity than a single crystal, it has in fact been observed without exception¹¹⁻¹³ that polycrystalline carbides have larger electrical conductivities than single crystals. For instance, if, by comparison with Fig. 4 we assume Taylor's sample with $x=0.95$ has a lattice component of $\kappa_p \approx 0.16 \text{ W cm}^{-1} \text{ K}^{-1}$, then $\kappa_e \approx 0.11 \text{ W cm}^{-1} \text{ K}^{-1}$ for his sample at 300 K. From the Wiedemann-Franz law, this corresponds to $\rho = 67 \mu\Omega \text{ cm}$, which agrees quite well with Taylor's reported value of $\rho = 60 \mu\Omega \text{ cm}$ at 273 K.

While the decrease in lattice thermal conductivity with temperature at high temperatures is not unexpected, the strength of the falloff is much weaker than the $1/T$ law expected from phonon-phonon umklapp processes. Klemens¹⁴ has developed a theory for the high-temperature lattice thermal conductivity when scattering by point defects is stronger than that of U processes, and shows that the expected temperature dependence is given by $\kappa_p \sim (AT)^{-0.5}$, where A is proportional to the strength of the point-defect scattering. We see in Fig. 4 that our results for TiC_x are qualitatively consistent with this result, with respect to both temperature and vacancy (point-defect) concentrations.

We turn now to Fig. 3 and a discussion of the thermopower of our samples. As we mentioned earlier, if phonon-drag effects are completely suppressed in these samples due to the large electron-vacancy scattering rate, the thermopower should be completely of the diffusion type. While one expects, based on a free-electron model, a diffusion thermopower S that varies linearly with temperature, this is not the case in many systems, including the present one. The most abundant examples occur in the realm of amorphous alloys¹⁵⁻²⁰ where the lack of any periodic crystal structure guarantees the absence of phonon drag. The thermopower of these materials generally exhibits a hump, or bend, around 50 K, a behavior that is well understood on the basis of renormalization of the electrons' energy (the so-called mass enhancement effect), velocity, and scattering rate due to their interaction with phonons. Opsal, Thaler, and Bass²¹ first introduced the concept as a mass enhancement of the thermopower in aluminum. The form of the enhancement is the same $(1+\lambda)$ mass enhancement that occurs in superconductors, where λ is the dimensionless electron-phonon coupling constant. In fact, mass enhancement effects have been invoked to explain the nonlinear thermopower of several Chevrel-phase superconductors,²² and it has even been suggested that such an effect may occur in the thermopower of high- T_c materials.^{23,24} Since the family of transition-metal carbides and nitrides all have relatively large electron-phonon coupling constants²⁵ (even though some of them, such as TiC , are not superconductors), one might expect that such effects may be manifest, especially in view of the strong electron-vacancy scattering that ensures the absence of phonon drag. Recently, in fact, mass enhancement effects were reported in the thermopower of polycrystalline NbN films.²⁶ We thus consider first the possibility that such enhancement effects may be active in TiC .

Kaiser²³ has shown that electron-phonon renormalization effects lead to a thermopower of the form

$$S = X_b T + a T \lambda_s(T), \quad (2)$$

where $X_b T$ is the bare diffusion thermopower in the absence of renormalization, and $\lambda_s(T)$ is the temperature-dependent enhancement factor given by

$$\lambda_s(T) = \frac{\int dE \alpha^2 F(E) G_s(E/k_B T)/E}{\int dE \alpha^2 F(E)/E}, \quad (3)$$

where $\alpha^2 F(E)$ is the Eliashberg function, $F(E)$ being the phonon density of states. The function $G(E/k_B T)$ has been given earlier by Kaiser.²⁷ The constant a in Eq. (2) is given by

$$a = \lambda(X_b + 2\beta + \gamma). \quad (4)$$

If only mass enhancement (energy renormalization) effects occur without any renormalization of the electron velocity and relaxation time, then $a = \lambda X_b$. The parameter 2β measures the strength of velocity and scattering time renormalization, and γ is a term due to higher-order diagrams (Nielsen-Taylor effect).

We can fit our thermopower curves using Eq. (2) with X_b and a as adjustable parameters. Since the form of the Eliashberg function is not known for TiC , we use $\alpha = \text{const}$ and a Debye $F(E)$. It turns out that the fit is not terribly sensitive to the particular form of $\alpha^2 F(E)$. For Debye temperature we use $\Theta = 740 \text{ K}$ from specific-heat data.²⁸ It is possible using this model to reproduce rather well the qualitative features of the data; see Fig. 3. The best fit requires $X_b = 11 \text{ nV K}^{-2}$ and $a = 33 \text{ nV K}^{-2}$. An estimate of λ for TiC is 0.25.²⁵ Thus $a/\lambda \approx 133 \text{ nV K}^{-2} \gg X_b$, implying that the observed enhancement cannot be accounted for on the basis of energy renormalization alone. In fact, $X_b \lambda \approx 2.8 \text{ nV K}^{-2}$, which means we require $(2\beta + \gamma)\lambda \approx 30 \text{ nV K}^{-2}$. This factor is on the order of that found by Kaiser *et al.* for NbN films; we believe, however, that such values for momentum and relaxation-time renormalization seem artificially large and unphysical.

We will show now that a mechanism considered originally by Lye⁷ to describe his thermopower data on TiC single crystals above 100 K is capable of explaining the present data throughout the entire temperature range, as well as providing an alternative explanation of the observed thermopower of NbN films. This approach is based on Mott's model of transport in transition metals.²⁹ The rather limited temperature range of Lye's study and the large scatter in the data prevented a detailed analysis in that case. We shall carry out such an analysis here, proceeding as follows. As is shown by Lye, based on the usual solution of the transport equation for an isotropic metal,³⁰ the thermopower can be written as

$$S^{-1} = S_1^{-1} + S_c^{-1}, \quad (5)$$

where S_1 is the part of the diffusion thermopower that is linear in temperature, $S_1 = AT$, and S_c , the correction to the linear thermopower, depends on various derivatives of the conductivity σ with respect to energy. Following Lye the second term can be written

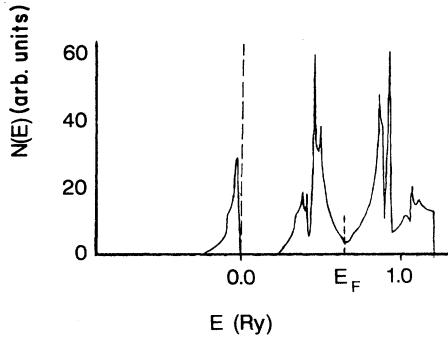


FIG. 5. Density of states of TiC, adapted from Ref. 31. Note the location of the Fermi energy E_F very near a minimum.

$$S_c = B(T/T_m + T_m/T), \quad (6)$$

where

$$B = (2\pi k/e)(\sigma'''/6\sigma')^{1/2}[\sigma''/\sigma' - \sigma\sigma'''/(\sigma')^2]^{-1} \quad (7)$$

and

$$T_m = (1/\pi k)(6\sigma'/\sigma''')^{1/2}, \quad (8)$$

where the derivatives of σ are with respect to energy and evaluated at the Fermi energy E_F . Now according to Mott's model, if the current-carrying electrons are scattered strongly by vacancies into the d band, then the conductivity is proportional to the d -band density of states (DOS); thus conductivity derivatives translate directly into derivatives of the d -band DOS at the Fermi level. It is when these derivatives are large that corrections to the simple proportionality between S and T become significant. This is precisely the situation in TiC, as is illustrated in Fig. 5. Here the calculated DOS for TiC is displayed;³¹ we see that E_F occurs very near a minimum in the d -band DOS, making it highly likely that higher-order conductivity derivatives are large, and lending support to the applicability of this model to the present case.

We have fitted our thermopower data over the entire temperature range to Eq. (5) using A , B , and T_m as adjustable parameters. The results for the $x=0.88$ sample are shown in Fig. 6; a similarly good fit is obtained for the other two samples. The parameters that give the best

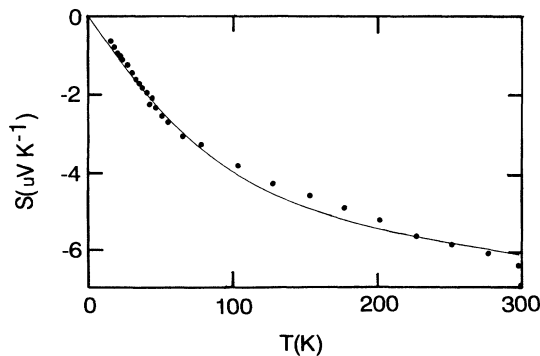


FIG. 6. Thermopower of TiC single crystals with $x=0.88$. A fit to the data using the s - d scattering model is indicated with a solid line.

TABLE II. Fitting parameters for the thermopower of TiC single crystals according to Mott's theory for s - d scattering.

Sample No.	x	A ($\mu\text{V K}^{-2}$)	B ($\mu\text{V K}^{-1}$)	T_m (K)
1	0.88	-0.05	-5.0	370
2	0.93	-0.05	-4.6	370
3	0.95	-0.05	-5.5	370

fit to the data are given in Table II. It is not possible to compare these values with those expected from electronic band-structure calculations because the conductivity derivatives at the Fermi level have not yet been evaluated. This perhaps could be the focus of future theoretical study.

While electron-phonon enhancement effects are capable of producing nonlinear thermopowers such as those observed here and in NbN films, it seems to us that the values of the parameters required to produce a good fit are unreasonably large. Rather, we believe that, at least in the case of TiC, the results are better understood on the basis of s - d scattering as outlined above, and suggest that this may also give an adequate explanation of the NbN data as well without invoking any enhancement effects. The main requirement is the existence of a d band near the Fermi level into which the conduction electrons can scatter.

SUMMARY

We have measured the thermal conductivity and thermoelectric power of TiC single crystals with $x=0.88$, 0.93, and 0.95, from 15 to 300 K. These measurements cover previously unexplored temperature regimes of thermal transport in these systems. Strong scattering of electrons by vacancies in this material produces a relatively large and weakly temperature-dependent resistivity. The electronic thermal conductivity is also substantially depressed due to vacancy scattering, accounting for at most 25% of the total heat conduction at room temperature and less than 5% below 100 K. The lattice thermal conductivity is limited by scattering from carbon vacancies at high temperature and electrons at low temperature. This produces a characteristic temperature dependence in which κ_p increases with increasing x above 100 K and decreases with increasing x below this temperature. The thermoelectric power is of the diffusion type, yet displays a "bend" around 60 K. This behavior can be quantitatively understood in terms of scattering of the transport s electrons into the d band, a process suggested originally by Lye in 1965 for TiC. It is proposed that the thermopower of other carbides and nitrides that possess a d band near the Fermi level can be understood in these terms as well.

ACKNOWLEDGMENTS

I would like to thank Dr. J. P. Heremans for a critical reading of the manuscript, Dr. T. A. Perry for enlightening discussions, and Anthony Gentile for supplying the samples.

- ¹L. E. Toth, *Transition Metal Carbides and Nitrides* (Academic, New York, 1971).
- ²W. S. Williams, *Phys. Rev.* **135**, A505 (1964).
- ³S. Otani, T. Tanaka, and Y. Ishizawa, *J. Mater. Sci.* **21**, 10 100 (1986).
- ⁴L. G. Radosevich and W. S. Williams, *Phys. Rev.* **181**, 181 (1969).
- ⁵L. G. Radosevich and W. S. Williams, *J. Am. Ceram. Soc.* **53**, 30 (1969).
- ⁶R. E. Taylor, *J. Am. Ceram. Soc.* **44**, 525 (1961).
- ⁷R. G. Lye, *J. Phys. Chem. Solids* **26**, 407 (1965).
- ⁸EPOTEK H20E, Epoxy Technologies, Billerica, MA.
- ⁹EPOTEK H72, same manufacturer.
- ¹⁰R. B. Roberts, *Philos. Mag.* **36**, 91 (1977).
- ¹¹J. Piper, *J. Appl. Phys.* **33**, 2394 (1962).
- ¹²J. Piper, in *Compounds of Interest in Nuclear Reactor Technology*, Institute of Metals Division Special Report No. 3, edited by P. Chiotti and W. N. Miner (Edwards, Ann Arbor, MI, 1964).
- ¹³F. A. Modine, M. D. Foegelle, C. B. Finch, and C. Y. Allison, *Phys. Rev. B* **40**, 9558 (1989).
- ¹⁴P. G. Klemens, *Phys. Rev.* **119**, 507 (1960).
- ¹⁵B. L. Gallagher, *J. Phys. F* **11**, L207 (1981).
- ¹⁶A. B. Kaiser, *J. Phys. F* **12**, L223 (1982).
- ¹⁷B. L. Gallagher, A. B. Kaiser, and D. Greig, *J. Non-Cryst. Solids* **61-62**, 1231 (1984).
- ¹⁸Z. Altounian, C. L. Foiles, W. B. Muir, and J. O. Strom-Olsen, *Phys. Rev. B* **27**, 1955 (1983).
- ¹⁹A. B. Kaiser, R. Harris, and B. G. Mulimani, *J. Non-Cryst. Solids* **61-62**, 1103 (1984).
- ²⁰J. Erwin, R. Delgado, H. Armbruster, D. G. Naugle, D. P. Love, F. C. Wang, C. L. Tsai, and T. O. Callaway, *Phys. Lett.* **100A**, 97 (1984).
- ²¹J. L. Opsal, B. J. Thaler, and J. Bass, *Phys. Rev. Lett.* **35**, 1211 (1976).
- ²²A. B. Kaiser, *Phys. Rev. B* **35**, 4677 (1987).
- ²³A. B. Kaiser, *Phys. Rev. B* **37**, 5924 (1988).
- ²⁴A. B. Kaiser and G. Mountjoy, *Phys. Rev. B* **43**, 6266 (1991).
- ²⁵U. Haufe, G. Kerker, and K. H. Bennemann, *Solid State Commun.* **17**, 321 (1975).
- ²⁶S. Reiff, R. Huber, P. Ziemann, and A. B. Kaiser, *J. Phys. Condens. Matter* **1**, 10 107 (1989).
- ²⁷A. B. Kaiser, *Phys. Rev. B* **29**, 7088 (1984).
- ²⁸W. S. Williams, *J. Am. Ceram. Soc.* **49**, 156 (1966).
- ²⁹N. F. Mott and H. Jones, *Theory of the Properties of Metals and Alloys* (Oxford University Press, Oxford, 1936), p. 267.
- ³⁰A. H. Wilson, *Theory of Metals* (Cambridge University Press, Cambridge, 1953), p. 204.
- ³¹A. Neckel, P. Rastl, R. Eibler, P. Weinberger, and K. Schwarz, *J. Phys. C* **9**, 579 (1976).